Advances in Nano Research, *Vol. 14, No. 5 (2023) 451-461*
https://doi.org/10.12989/anr.2023.14.5.451

A design of tuning band and structure to generate diverse properties by stretching

Ruqi Wang*[1] and Ruoyun Li[2]

[1]*College of Chemistry and Chemical Engineer*, *Lanzhou University*
[2]*Institute of Biochemistry and Molecular Biology*, *School of Life Sciences*, *Lanzhou University*

(*Received February 6, 2022, Revised June 12, 2022, Accepted June 28, 2022*)

Abstract. Two-dimensional (2D) materials have been attracting attention since graphene monolayer was firstly separated. However, after an explosive boom, there is always quandary and stagnancy following and soon will come the refractory period of capital market. To avoid that undesired future, a paradigm of quasi 2D monolayer has been contemplated and devised in this article, with examples studied theoretically. The results show the general dynamic nonlinearity, and the expected tunability of bandgap without extra doping or substitution. These together suggest its intriguing both electronical and mechanical properties, which will enrich the arsenal of potential 2D materials.
Keywords: double-deck interlaced structure; high information density; mechanical non-linearity; post-preparation bandgap engineering; quasi-2D-monolayer; strain-induced haptotropic shift

;

1. Introduction

In recent years, the research on preparation, characterization and application of 2D materials has shown a blowout rise due to the diversity of existing and promising structures and modification methods (Han *et al*. 2007, Mccann 2007, Arne *et al*. 2008, Topsakal *et al*. 2009, Zhi *et al*. 2009, Duong *et al*. 2012, Huang *et al*. 2013, Li *et al*. 2014b, Ye *et al*. 2014, Tan and Zhang 2015, Zhou *et al*. 2015, Lin and Lin 2017, Cao *et al*. 2018, Hailong *et al*. 2018, He *et al*. 2019). Since the first separation of graphene monolayer in 2004 (Novoselov *et al*. 2004), 2D materials have attracted wide attention due to unique properties. Whereas graphene exhibits superb electrical, thermal, and mechanical properties, its metallic band limits the application potentiality (Schwierz 2010, Gao *et al*. 2021, Yang *et al*. 2021, Hao *et al*. 2022, Peng *et al*. 2022, Xin *et al*. 2022).

Subsequently, tremendous interest has been focused on the development of analogous 2D materials, such as hexagonal boron-nitride (Topsakal *et al*. 2009, Zhi *et al*. 2009, Hong *et al*. 2021, Wu *et al*. 2021, Xi *et al*. 2021, Shi *et al*. 2022, Xu *et al*. 2022), transition metal dichalcogenides (Huang *et al*. 2013, Tan and Zhang 2015), black phosphorus (Li *et al*. 2014b), graphitic carbon-nitride (g-C3N4) (Arne *et al*. 2008). Meanwhile, various approaches to modifying electronic structure and band configuration have been contrived, mainly based on heteroatomical doping (Zhou *et al*. 2015), morphological controlling (Han *et al*. 2007, Mccann 2007, Duong *et al*. 2012, Cao *et al*. 2018, Hailong *et al*. 2018), substituent functionalization (Ye *et al*. 2014, Lin and Lin 2017), combination and copolymerization (He *et al*. 2019), et cetera. However, demanding efforts are often required for different materials and multiple processes, which consequently limit the academical development and commercial application of 2D materials. Take doping and codoping of graphene as an example, simple permutation and combination shows that, the total number of combinations increases exponentially with codopant species. Such endless attempts reflect a certain level of serendipity and blindness (Wang *et al*. 2020a, Fan *et al*. 2022, Wang *et al*. 2022a, Xia *et al*. 2022). Moreover, current bandgap engineering methods are mainly limited to preparation or construction stage (Han *et al*. 2007, Mccann 2007, Arne *et al*. 2008, Duong *et al*. 2012, Ye *et al*. 2014, Zhou *et al*. 2015, Lin and Lin 2017, Cao *et al*. 2018, Hailong *et al*. 2018, He *et al*. 2019). That is to say, each new material is forged into specific property relying on its native structure, with mere flexibility and adaptability (Shengchun *et al*. 2016).

Strain engineering is a common method to improve that, by tuning structural parameters thus to perturb the band configuration (Sharma *et al*. 2003, Guinea *et al*. 2009, Jiao *et al*. 2015, Roldán *et al*. 2015, Naumis *et al*. 2017). This method can be used to tune the electronic and photonic performance afterwards, routinely in manufacturing semi-conductor devices (Li *et al*. 2014a, Liu *et al*. 2020, Wang *et al*. 2020b, Zhou *et al*. 2020, Dai *et al*. 2021, Guo *et al*. 2021, Shao *et al*. 2021, Wu and Habibi 2021). While in organometallic frames with finer structures, it is likely to have more complex changing patterns with strain (Ma *et al*. 2022, Zhao *et al*. 2022, Hou *et al*. 2021, Huang *et al*. 2021a, Huang *et al*. 2021b, Jiao *et al*. 2021, Liu *et al*. 2021, Moradi *et al*. 2021, Xu *et al*. 2021, Dong *et al*. 2022, Luo *et al*. 2022, Michael *et al*. 2022, Wang *et al*. 2022b, Yang *et al*. 2022, Yu *et al*. 2022).

In a non-rigid body, cross-sections will slide in parallel under shear force. Similarly for sandwich complexes,

*Corresponding author, Ph.D.,
E-mail: grq2016@lzu.edu.cn

ISSN: 2287-237X (Print), 2287-2388 (Online)

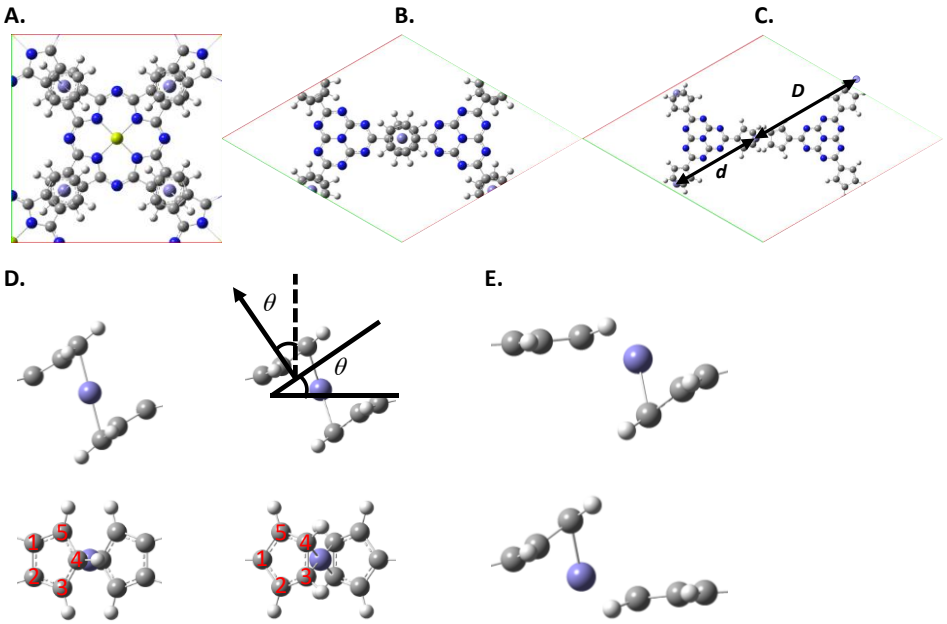

Fig. 1 Ball-and-stick models of examples; (a) Relaxed structure of the tetragonal example; (b) Relaxed structure of the hexagonal example in P-3m1; (c) Structure of the hexagonal example with deviation in P3m1; (d) Sandwich complex moiety without deviation, € Side views of a pair of symmetrical sandwich complex moieties

haptotropic shift (O'Connor and Casey 1987, Veiros and Luis 2012) with molecular deflection and ligand slippage will occur, when a pair of anti-parallel and non-collinear forces (shear force) acts on ligands at both ends. And when both ligands in each complex form conjugated organic linkers respectively, the coplane of such linkers will bend and restore under stress. The synergy of haptotropic shift and coplane deformation will lead to complex structural changes and the system nonlinearity. The electronic structure will consequently transform, and for a periodic system, the band configuration will change (Dai and Safarpour 2021, Forsat *et al*. 2021, Ghamkhar *et al*. 2021, Khadimallah *et al*. 2021a, b, Kumar *et al*. 2021, Madenci 2021, Tlidji *et al*. 2021).

Accordingly, a paradigm utilizing this synergy was designed. The quasi 2D metal-organic frameworks (MOFs) of this paradigm (Fig. 1(a) and 1(b)) is constructed from sandwiched metallic nodes and threefold or fourfold symmetric organic linkers. In such structure, film tension can be transferred through linkers and applied on sandwiched metallic nodes as shear force, which will force the haptotropic shift, while in planar MOFs, the film tension cannot form such shear force due to its coplanarity. It is noteworthy that quasi refers to the tunable double-deck interlaced arrangement of organic linkers (Fig. 1(a) and 1(b)), rather than a oligo-repetition on the third dimension perpendicular to film plane (e.g., quasi 2D perovskite (Tsai *et al*. 2016, Zheng *et al*. 2018, Zhou *et al*. 2018)), therefore the overall structure is still a monolayer.

Following such paradigm, we calculate two examples to illustrate it (Fig. 1(a) and 1(b)). Based on density functional theory (DFT), we investigate both electronical and mechanical properties of typical structures, including bandgap changing, stress-strain relationship and energy landscape. The deformation of energy landscape under external electric fields (EEF) has also been determined for further exploitation.

2. Method

2.1 Modeling

Two examples are designed (Fig. 1(a) and 1(b)) according to the forementioned paradigm. Structures are detailedly defined as follows for further discussion. The hedral angle θ between ligand ring and horizontal plane is defined as the angle between vertical vector and normal vector of ligand ring (Fig. 1(d)), while the normal vector is defined as the average of cross products of each pair of adjacent C-C bond vectors in tandem. Deviation rate is defined by *r*, while *d* is defined as the distance between two Fe ions in one cell, and *D* is defined as the shortest distance between two Fe ions in two adjacent cells (Fig. 1(c)). Plus-minus is used to distinguish a pair of symmetrical structures. $r = 0$ refers to the structure in P-3m1 group with no deviation of Fe ions (Fig. 1(d)), while $r = \pm 1$ refers to a pair of symmetrical structures in P3m1 group (Fig. 1(e)).

The combination of deviations generates more structures in lower space groups. For structures with lower symmetry, here $r = 0, \pm 1$ refers to three potential energy extrema respectively. With a proper lattice parameter *a*, three stable states in P-3m1 and P3m1 groups exist with identical free energy. Therefore maintaining the translational symmetry of adjacent lattices, there will be $3^3 = 27$ different combinations with similar energy, which can be presented in the form as (r_1,r_2,r_3) and divided into six degenerate groups (0,0,0) (i,i,i) (0,0,i) (0,i,i) (i,i,-i) (0,i,-i) as shown with a polynomial below:

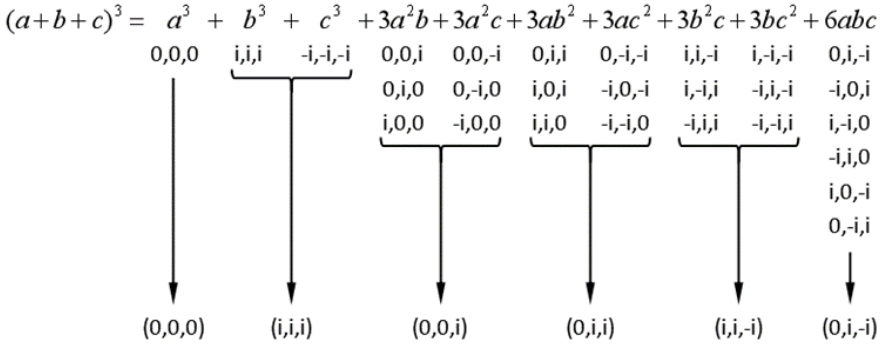

(1)

States in one group are symmetrical to each other, yet considering the interplay among connected ferrocene moieties, free energy of different groups will not be exactly identical. Similarly for *a* with two stable states (), there will be $2^3 = 8$ combinations in two degenerate groups (i,i,i) (i,i,-i) correspondingly (Habibi *et al*. 2016, 2018a, b, 2019b, d, e, Ebrahimi *et al*. 2019, Esmailpoor Hajilak *et al*. 2019, Pourjabari *et al*. 2019, Safarpour *et al*. 2019a, Zhu *et al*. 2022).

In order to estimate the photoelectric conversion efficiency of a pile of monolayers with decreasing bandgap gradient in vertical direction from top to bottom, the detailed equilibrium limit formula (1) (Shockley and Queisser 1961) is extended to fit for multi-junction (2) and bandgap gradient multilayer (3) device as follows.

$$\eta = FF \cdot \frac{k_B T}{hc} \ln\left(\frac{\int_0^{\lambda_g} I_{\odot}(\lambda)\lambda \mathrm{d}\lambda}{\int_0^{\lambda_g} I_{300\mathrm{K}}(\lambda)\lambda \mathrm{d}\lambda} - 1\right) \frac{\int_0^{\lambda_g} I_{\odot}(\lambda)\lambda \mathrm{d}\lambda}{\int_0^{\infty} I_{\odot}(\lambda)\mathrm{d}\lambda} \quad (2)$$

FF = filling factor

λ_g = Wavelength of the photon with same energy as bandgap

$I_{300K}(\lambda)$ = Irradiance distribution versus wavelength of black body at 300K

$I_{\odot}(\lambda)$ = Irradiance distribution versus wavelength of solar spectrum at sea level (Testing *et al*. 2008)

$$\eta = \frac{FF \cdot k_B T}{hc \int_0^{\infty} I_{\odot}(\lambda) d\lambda} \sum_{i=1}^{n} ln\left(\frac{\int_{\lambda_{i-1}}^{\lambda_i} I_{\odot}(\lambda)\lambda d\lambda}{\int_{\lambda_{i-1}}^{\lambda_i} I_{300K}(\lambda)\lambda d\lambda} - 1\right) \int_{\lambda_{i-1}}^{\lambda_i} I_{\odot}(\lambda)\lambda d\lambda \quad (3)$$

λ_n = Wavelength of the photon with same energy as bandgap of each layer.

$$\eta = \frac{FF \cdot k_B T}{hc \int_0^{\infty} I_{\odot}(\lambda) d\lambda} \times \left[ln\left(\frac{\int_0^{\lambda_{\min}} I_{\odot}(\lambda)\lambda d\lambda}{\int_0^{\lambda_{min}\int} I_{300K}(\lambda)\lambda d\lambda} \int_0^{\lambda_{min}\int_{\lambda_{min}}^{\lambda_{max}\int} ln\left(\frac{I_{\odot}(\lambda)}{I_{300K}(\lambda)}-1\right) I_{\odot}(\lambda)\lambda d\lambda} I_{\odot}(\lambda)\lambda d\lambda\right)\right] \quad (4)$$

$\lambda_{ma\ x}$ = Wavelength of the photon with same energy as bandgap of bottom layer

λ_{min} = Wavelength of the photon with same energy as bandgap of top layer

2.2 Computational methods

The optimization and band calculations (Habibi *et al*. 2017, Safarpour *et al*. 2018, Habibi *et al*. 2019a, Habibi *et al*. 2019c, Safarpour *et al*. 2019b, Alipour *et al*. 2020, Ebrahimi *et al*. 2020, Ghazanfari *et al*. 2020, Safarpour *et al*. 2020, Chen *et al*. 2022) are based on DFT with the projector-augmented wave (PAW) method utilizing the Vienna ab initial Simulation Package (VASP) (Zupan *et al*. 1997, Rocha *et al*. 2006, Rungger and Sanvito 2008). The exchange-correlation potential is treated at the generalized gradient approximation (GGA) using the Perdew-Burke-Ernzerhof (PBE) functional (Hammer *et al*. 1999). For all calculations the PREC-tag is set Accurate, therefore the cutoff energy for the plane-wave basis set is 500 eV. Lattice parameters *a b* are set identical and increasing at 0.2 Å intervals in order to maintain planar tetragonal or hexagonal cell for scanning, while the parameter *c* is set 20 Å, which makes a sufficient vacuum layer to avoid the interaction between adjacent layers. The k-point mesh is set to 1×1×1 for the first Brillouin zone, since the resolution is high enough for lattice of this size. Dipole corrections (Pederson and Jackson 1991, Makov and Payne 1995) perpendicular to the vacuum layer are performed for hexagonal cells, since a net dipole moment is generated due to symmetry-breaking of structures in P3m1 group, and such corrections are requisite for calculations with EEF. Fermi-smearing with a width of σ = 0.12 eV is used in all calculations, for a bigger or smaller smearing width leads to either excessive electron entropy or energy non-convergence with larger lattice parameters. Geometry optimization are performed for all structures to minimize the Hellmann-Feynman forces with a tolerance of 0.01 eV/Å. The criterion of energy convergence is set to $1*10^{-7}$ eV.

3. Results and discussion

Optimization of a ferrocene molecule is firstly performed in the same condition to verify the reliability of computational methods. The resulting length of the C-C bond is 1.43 Å, and the distance between two Cps is 3.29 Å, which are consistent to experimental values of 1.43 Å and 3.32 Å (Bohn and Haaland 1966), therefore the conclusion can be drawn that the calculation method in this work is accurate enough.

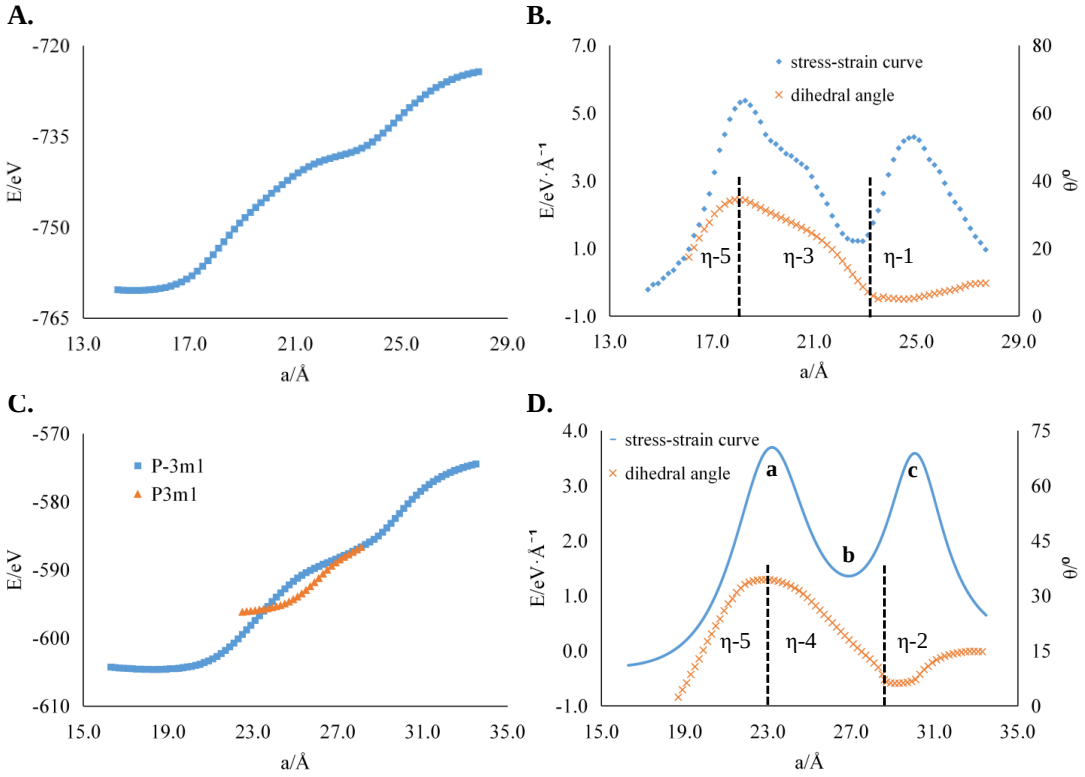

Fig. 2 Energy-strain&stress-strain relationships with dihedral angle changing; (a), (b) Energy-strain and stress-strain scatter of tetragonal example; (c) Energy-strain scatter of P-3m1 and P3m1 structures; (d) Stress-strain relationship derived from energy-strain scatter of P-3m1 structure, dihedral angles are derived from the coordinates of optimized structures. For ab section in stress-strain curve, the energy decline caused by coplane recovery partially counteracts the trend of accelerating energy increase, causing a temporary decline of stress; For bc section, coplane recovery no longer compensates the energy increase acceleration of ligand separation, and finally after c point trend of energy increase begins to slow down

Following the paradigm, two examples are designed and calculated, with the results reflecting the expected synergy. The number and the deviation rate of stable structures vary with *a* in the hexagonal example, manifesting different cross-sections of energy landscape, which may be suitable for various purposes such as information storage, high-performance computing, catalysis and adsorption. With increasing *a*, the bandgap of P-3m1 group declines continuously, which shows prominent potential for photoelectric conversion.

3.1 The optimization of tetragonal structure in P4/nmm group

With *a b* close to 15.1 Å, the structure reaches its minimum energy, and phthalocyanine-like organic linkers (magnesium (II) tetracyclopentadienoporphrazine anion, $MgTCpPz^{4-}$) are almost coplanar (Fig1.A). As *a* increases, the originally overlapped Cp rings in each ferrocenyl moiety slip oppositely, and haptotropic shift occurs in each ferrocenyl moiety. In the meantime, planes of each linker are bent at first and then partially recover, then bent slightly and recover again, consistent with a process from η-5 to η-3 and then to η-1 coordination of Cp rings.

The stress-strain scatter plot is obtained by the difference of the energy-strain scatter plot. In the early stage of stretching, the trends of stress and the dihedral angle are mutually consistent (Fig2). From η-5 to η-3, C1 and C2 first stick to Fe ion and then abandon, causing a decline in dihedral angle, the energy decline caused by coplane recovery partially counteracts the trend of accelerating energy increase. From η-3 to η-1, C3 and C5 also abandon, with a drop in dihedral angle. In η-1 zone dihedral angle increases again due to interactions between Fe ions and C-H bonds.

3.2 The optimization of hexagonal structure in P-3m1 group

With *a b* close to 18.3 Å, the structure reaches its minimum energy. The stretching process is similar to the previous. However, due to the different connection between the ligand loop and the body of linker, the haptotropic shift process is accordingly from η-5 to η-4 and then to η-2 (Fig. 2(b)).

Due to a poor polynomial fitting result for energy-strain scatter, a more reasonable model is necessary. Here we fit the scatter using a set of arc-tangent functions ($R^2 = 0.99997$), and obtain the stress-strain relationship by derivation (Fig. 2(b)). The wavelet of dihedral angle change is consistent with the hollow of stress-strain curve (Fig. 2(b)), indicating that the recovery of coplane counteracts

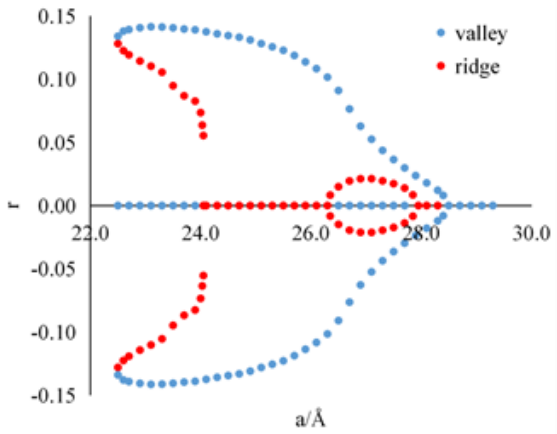

Fig. 3 Valleys and ridges of energy landscape. The r of the optimized structures changes with a. Tracking r of stable and transition states, the valleys and ridges of energy landscape versus a and r were manifested. Valley means the minimum of energy, while ridge shows maximum. presents the structure of P-3m1

the energy increase caused by ligand separation, which explains the peculiar fluctuant growth relationship of free energy (Fig. 2(a)).

As the stress-strain relationship shows non-monotonicity, within a range of strain, a has multiple solutions for each different stress. Thus, it can be extrapolated that a mixture of organic linkers with different stretch ratio can also reach a mechanical equilibrium state (Fig. 1(c)). Therefore, we performed further optimization to search potential stable states in a lower space group (P3m1).

3.3 The optimization of structures in the P3m1 space group

With each *a* ranging from 22.5 to 28.6 Å, a pair of energy minimum states in the P3m1 space group has been spotted (Fig. 1(c)). According to symmetry, two structures of each pair with $r = \pm 1$ are identical in morphology and energy. For structures in the P-3m1 space group, it is always accordingly $r = 1$.

In the meantime, symmetry breaking from P-3m1 to P3m1 group produces a dipole moment. The existence of vertical component of dipole moment indicates EEF might change the energy and conformation of structures, thus we performed further calculations under EEF to reveal that.

3.4 Energy landscape

The *r* of the optimized structures changes with *a*. In order to reflect the complicated energy landscape, *r* of stable and transition a state has been tracked (Fig. 3), to manifest valleys and ridges of energy landscape versus *a* and *r*. According to energy-strain scatter and energy landscape, transverse cross-sections with scanned *r* and three designedly chosen *a* (*a* = 23.60 Å, 25.10 Å and 24.00 Å) are calculated (Fig. 4.A).

For *a* = 23.60 Å, free energy of three stable states in P-3m1 and P3m1 groups is identical, generating 27 combinations in 6 degenerate groups (See modeling).

Theoretically, each lattice carries $\log_2 27 = 4.75$ bit information, similar to that carried by one synapse in human brain (Bartol *et al*. 2015). For each group, optimization and energy calculation are performed, and free energy is respectively $E_{(0,0,0)}$ = -595.71 eV, $E_{(i,i,i)}$ = -595.72 eV, $E_{(0,0,i)}$ = -596.62 eV, $E_{(0,i,i)}$ = -597.08 eV, $E_{(i,i,-i)}$ = -595.74 eV, $E_{(0,i,-i)}$ = -597.10 eV. The free energy of group (0,i,i) and (0,i,-i) is almost identical and significantly lower than that of other groups, indicating information carried in each lattice is less than 4.75 bit and more than $\log_2 12 = 3.58$ bit. Even still, a $1cm^2$ piece of such monolayer can carry information two orders of magnitude higher than that in a human brain.

For *a* = 25.10 Å, there are two P3m1 stable structures symmetrical to each other with notable energy barrier, generating 8 combinations in two degenerate groups (See modeling). Free energy of each group is respectively -593.93 and -593.96 eV, therefore each lattice carries about $\log_2 6 = 2.58$ to $\log_2 8 = 3$ bit information. Judging from valleys and ridges (Fig. 3), from *a* = 24.10 to 26.10 Å, the cross-section shows a single peak similar to the energy profile of a magnetic tunnel junction (MTJ), which has been proved available as stochastic building blocks for probabilistic computing (Borders *et al*. 2019). Furthermore, the energy barrier from 0.37 to 0.91 eV (equivalent to 14 to 35 kT_{300K}) is suitable for probabilistic computing (Borders *et al*. 2019), indicating ferrocenyl moieties may also serve as building blocks.

As for *a* = 24.00 Å, a plateau in the cross-section as expected indicates a gentle relaxation process and a continuous change of electronic structure, which suggests its potential for varied catalysis and adsorption process (Zhang *et al*. 2019).

3.5 Energy cross section transformation with extra electric field (EEF)

A uniform deviation leads to the symmetry breaking from P-3m1 to P3m1 group, and for electronic structure, such symmetry breaking produces dipoles perpendicular to the film, causing orientation preference for each ferrocenyl moiety under vertical EEF, which means a deformation and deviation of energy cross-section. Therefore cross-section under EEF are calculated (Fig. 4.B, C).

For both chosen *a* 23.60 and 25.10 Å, one side of P3m1 structure becomes thermodynamically more stable and kinetically preferred under EEF, while the other side becomes the opposite. And the transformation of cross-section becomes more remarkable with an enhanced EEF. It means that the deviation direction of Fe ion in the lattice can be manipulated with a sufficient EEF, indicating a possible method of information writing and rewriting.

3.6 Band calculation

For the first stress-strain monotonous interval, about 18.30 to 23.00 Å, the P-3m1 conformation is the only stable state, or thermodynamically much more stable than that in P3m1 group (Fig. 2). For larger *a*, there will be a mixture of

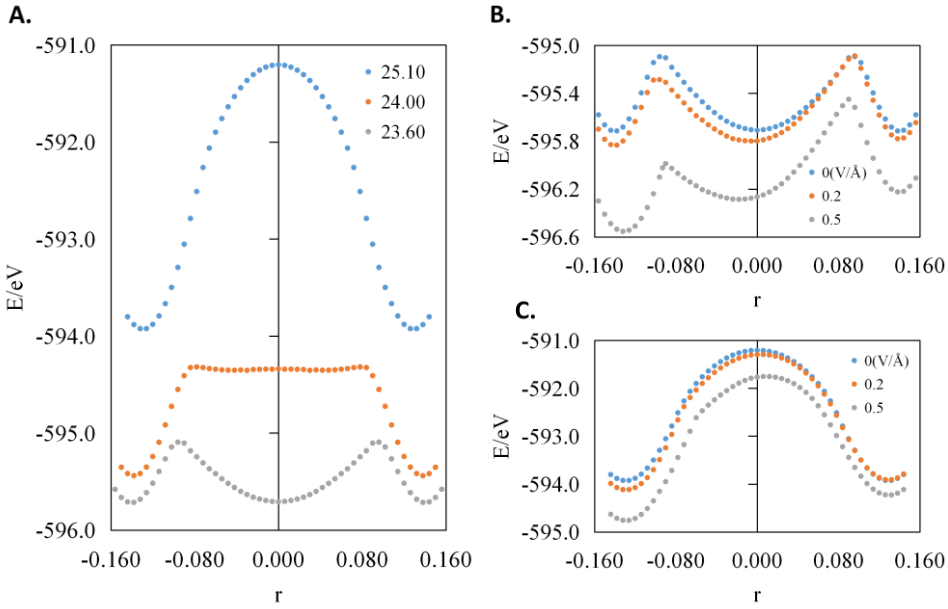

Fig. 4 Transverse cross-section of energy landscape with and without EEF. (a) Transverse cross-section of energy landscape with lattice parameters set 23.60, 24.00, and 25.10 Å. (b), (c) Cross-section transformation with extra electric field (0.2, 0.5 V/Å), taking a = 23.60 and 25.10 Å respectively as examples

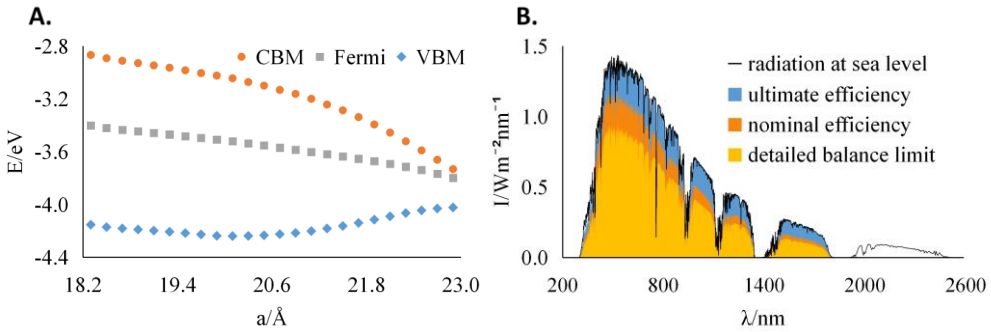

Fig. 5 Band change under tension and related application in solar cell; (a) Changes of conduction band minimum, Fermi level and valence band maximum (b) Theoretical photovoltaic efficiency with continuous bandgap using the same analysis method as in Shockly-Queisser limit, the proportion of the detailed balance limit part is the theoretical upper limit of actual efficiency, which is around 57.9%

P-3m1 and P3m1 states. Therefore focusing on the P-3m1 structure, band calculations are performed with scanned *a* within an interval from 18.30 to 22.90 Å, to reveal the bandgap change with different strains (Fig. 5(a)).

The results show a tunable bandgap ranging from 0.29 to 1.29 eV. However, the GGA-PBE functional is well known for its underestimation on bandgap of a semiconductor. For monolayer g-C3N4, the bandgap calculated by GGA-PBE functional is 1.2 eV, which is 1.5 eV smaller than the experimental value 2.7 eV (Shariati *et al*. 2023). With a proportional correction, the actual bandgap range should be around 0.65 to 2.89 eV, and an extra bandgap calculation by HSE06 functional obtain the upper limit at 2.79 eV. This notable change can be superficially explained as, with the slippage of Cp ring, C1 is gradually separated from Fe ion, distributing more orbital to the conjugation with carbon-nitride moiety rather than the coordination with Fe ion, therefore the mismatch of Fe orbital and the overall enhancement of conjugation in the whole system leads to the increasement of electrical conductivity.

Such a continuous change of electronic structure and bandgap is of prominent significance for applications as catalysis, photocatalysis and photoelectric conversion. Here we take its potential application for high-efficiency multi-junction solar cell as an example. As Shockley and Queisser deduced, the conversion efficiency of a solar cell is limited by a contradiction as the limited energy range of absorption versus the heat waste of absorbed photons (Shockley and Queisser 1961). The detailed balance limit of single junction solar cells can be calculated by equation 1 in method, and accordingly silicon heterojunction solar cells with a bandgap around 1.1 eV is close to maximum efficiency of 28% (Yoshikawa *et al.* 2017). On such basis, overlying junctions with decreasing bandgaps can cope with the range-rate contradiction to breach the of efficiency limit (equation 2), and successful attempts have been made for years (King *et al*. 2007), including a record of 47.1% set recently (Geisz *et al*. 2020). To further such break and maximize the utilization

of photon energy in the absorption range, a multilayer structure with decreasing bandgap gradient is devised. According to the extended formula (Eq. 3), we expect that with our calculated bandgap ranging from 0.65 to 2.89 eV and a moderate FF of 0.8, the efficiency of such multi-junction solar cell can be up to 57.9% (Fig. 5(b)), which is much higher than any existing record.

3.7 Potential modification and similar structure

Our work is mainly to develop and theoretically validate a facile method for band and structure tuning. Besides this part, classical modifications are still feasible in our paradigm. For example, in the hexagonal structure explicated above, doping in carbon-nitride moieties remains available, while comparing to original g-C3N4, extra substituent positions are introduced by ferrocenyl moieties, making it possible for functionalization and graft crosslinking modification. The pore size of a relaxed structure is slightly over 10 Å, which is dimensionally suitable for a buckyball, carbon nanotube, or nanoparticle to embed into. The size is also tunable by stretching, and the affinity of pores can be regulated by modification of substituent on ferrocenyl moieties.

Notice that in order to control variables, calculations in this article are mainly restricted to a relatively high space group, or at least with a consistent lattice. The real situation can be more complicated. The whole system may degenerate into a rectangular, orthorhombic or even aperiodic one with specific external force, which further highlights its mechanical non-linearity. A phenomenological network dynamic modeling and analysis are required in the following study since first principle study is overkill and incompetent at this level, but basically we expect a chaotic system with enough patterns and information, moderate energy barrier, and mechanical and photoelectric sensitivity to nurture intelligence (Liu *et al*. 2013, Merindol and Walther 2017)

The features discussed above are supposed to be prevalent in combinations following this paradigm, thus more structures can be devised. For instance, cerocene with triazine, dibenzene chromium with metallo-phthalocyanine, ferrocene with metalloporphyrin, et cetera. These structures and their change of band configuration will extremely enrich the arsenal of potential materials. Moreover, the tension can stabilize the originally unstable conformation of sandwich complex moiety, or even less strictly other elastically deformable moiety, which provides a new approach to study complex dynamical behaviors of such moiety.

4. Conclusions

In this article, we contemplated and devised a paradigm of structures with bandgap tunable by stretching. According to the examples calculated, the coupling of haptotropic shift of sandwich complex and the bending of conjugated coplanar lead to mechanical non-linearity and a tunable bandgap. To be specific, the hexagonal structure has a high information density with a moderate energy barrier, and a considerable bandgap range. It is worth mentioning that, more structures with similar features can be devised likewise. Such features provide the possibility to realize diverse catalytic reactions, achieve a full use of solar energy, and pave a new way to study the unstable conformation experimentally.

References

Alipour, M., Torabi, M.A., Sareban, M., Lashini, H., Sadeghi, E., Fazaeli, A., Habibi, M. and Hashemi, R. (2020), "Finite element and experimental method for analyzing the effects of martensite morphologies on the formability of DP steels", *Mech. Based Des. Struct.*, **48**(5), 525-541. https://doi.org/10.1080/15397734.2019.1633343

Bartol, T.M., Cailey, B., Justin, K., Chirillo, M.A., Bourne, J.N., Harris, K.M. and Sejnowski, T.J. (2015), "Nanoconnectomic upper bound on the variability of synaptic plasticity", *eLife Sci.*, **4**. https://doi.org/10.7554/eLife.10778

Bohn, R.K. and Haaland, A. (1966), "On the molecular structure of ferrocene, Fe(C5H5)2", *J. Organometall. Chem.*, **5**(5), 470-476. https://doi.org/10.1016/S0022-328X(00)82382-7

Borders, W.A., Pervaiz, A.Z., Fukami, S., Camsari, K.Y. and Datta, S. (2019), "Integer factorization using stochastic magnetic tunnel junctions", *Nature*, **573**(7774), 390-393. https://doi.org/10.1038/s41586-019-1557-9

Cao, Y., Fatemi, V., Fang, S., Watanabe, K., Taniguchi, T., Kaxiras, E. and Jarillo-Herrero, P. (2018), "Unconventional superconductivity in magic-angle graphene superlattices", *Nature*, **556**. https://doi.org/10.1038/nature26160

Chen, F., Chen, J., Duan, R., Habibi, M. and Khadimallah, M.A. (2022), "Investigation on dynamic stability and aeroelastic characteristics of composite curved pipes with any yawed angle", *Compos. Struct.*, 115195. https://doi.org/10.1016/j.compstruct.2022.115195

Dai, H. and Safarpour, H. (2021), "Frequency and thermal buckling information of laminated composite doubly curved open nanoshell", *Adv. Nano Res.*, **10**(1), 1-14. https://doi.org/10.12989/anr.2021.10.1.001

Dai, Z., Jiang, Z., Zhang, L. and Habibi, M. (2021), "Frequency characteristics and sensitivity analysis of a size-dependent laminated nanoshell", *Adv. Nano Res.*, **10**(2), 175. https://doi.org/10.12989/anr.2021.10.2.175

Dong, Y., Gao, Y., Zhu, Q., Moradi, Z. and Safa, M. (2022), "TE-GDQE implementation to investigate the vibration of FG composite conical shells considering a frequency controller solid ring", *Eng. Anal. Bound. Elem.*, **138**, 95-107. https://doi.org/10.1016/j.enganabound.2022.01.017

Duong, D.L., Lee, S.M., Chae, S.H., Ta, Q.H., Lee, S.Y., Han, G.H., Bae, J.J. and Lee, Y.H. (2012), "Band-gap engineering in chemically conjugated bilayer graphene: Ab initio calculations", *Phys. Rev. B*, **85**(20), 45-51. https://doi.org/10.1103/PhysRevB.85.205413

Ebrahimi, F., Habibi, M. and Safarpour, H. (2019), "On modeling of wave propagation in a thermally affected GNP-reinforced imperfect nanocomposite shell", *Eng. Comput.*, **35**(4), 1375-1389. https://doi.org/10.1007/s00366-018-0669-4

Ebrahimi, F., Hashemabadi, D., Habibi, M. and Safarpour, H. (2020), "Thermal buckling and forced vibration characteristics of a porous GNP reinforced nanocomposite cylindrical shell", *Microsyst. Technol.*, **26**(2), 461-473. https://doi.org/10.1007/s00542-019-04542-9

Esmailpoor Hajilak, Z., Pourghader, J., Hashemabadi, D., Sharifi Bagh, F., Habibi, M. and Safarpour, H. (2019), "Multilayer

GPLRC composite cylindrical nanoshell using modified strain gradient theory", *Mech. Based Des. Struct.*, **47**(5), 521-545. https://doi/10.1080/15397734.2019.1566743

Fan, L., Huang, Y., Ji, D., Moradi, Z., Safa, M. and Amine Khadimallah, M. (2022), "Interaction of angular velocity and temperature rise in the thermo-inertia bifurcation buckling of FG laminated nanocomposite annular plates", *Eng. Struct.*, **265**, 114518. https://doi.org/10.1016/j.engstruct.2022.114518

Forsat, M., Musharavati, F., Eltai, E., Zain, A.M., Mobayen, S. and Mohamed, A.M. (2021), "Vibration characteristics of microplates with GNPs-reinforced epoxy core bonded to piezoelectric-reinforced CNTs patches", *Adv. Nano Res.*, **11**(2), 115-140. https://doi.org/10.12989/anr.2021.11.2.115

Gao, T., Zhang, Y., Li, C., Wang, Y., An, Q., Liu, B., Said, Z. and Sharma, S. (2021), "Grindability of carbon fiber reinforced polymer using CNT biological lubricant", *Sci. Rep.*, **11**(1), 1-14. https://doi.org/10.1038/s41598-021-02071-y

Geisz, J.F., France, R.M., Schulte, K.L., Steiner, M.A. and Moriarty, T. (2020), "Six-junction III–V solar cells with 47.1% conversion efficiency under 143 Suns concentration", *Nature Energy*, **5**(4), 326-335. https://doi.org/10.1038/s41560-020-0598-5

Ghamkhar, M., Khadimallah, M.A., Iqbal, M.Z., Hussain, M., Yahya, A., Khedher, K.M., Naeem, M.N. and Tounsi, A. (2021), "Performance of FGM bilayered cylindrical shell placed on cantilever edge", *Adv. Nano Res.*, **11**(4), 339-345. https://doi.org/10.12989/anr.2021.11.4.339

Ghazanfari, A., Soleimani, S.S., Keshavarzzadeh, M., Habibi, M., Assempuor, A. and Hashemi, R. (2020), "Prediction of FLD for sheet metal by considering through-thickness shear stresses", *Mech. Based Des. Struct.*, **48**(6), 755-772. https://doi.org/10.1080/15397734.2019.1662310

Guinea, F., Katsnelson, M.I. and Geim, A.K. (2009), "Energy gaps and a zero-field quantum Hall effect in graphene by strain engineering", *Nature Phys.*, **6**(1), 30-33. https://doi.org/10.1038/nphys1420

Guo, J., Baharvand, A., Tazeddinova, D., Habibi, M., Safarpour, H., Roco-Videla, A. and Selmi, A. (2021), "An intelligent computer method for vibration responses of the spinning multi-layer symmetric nanosystem using multi-physics modeling", *Eng. Comput.*, 1-22. https://doi.org/10.1007/s00366-021-01433-4

Habibi, M., Ghazanfari, A., Assempour, A., Naghdabadi, R. and Hashemi, R. (2017), "Determination of forming limit diagram using two modified finite element models", *Mech. Eng.*, **48**(4), 141-144. https://doi.org/10.22060/MEJ.2016.664

Habibi, M., Hashemabadi, D. and Safarpour, H. (2019a), "Vibration analysis of a high-speed rotating GPLRC nanostructure coupled with a piezoelectric actuator", *Eur. Phys. J. Plus*, **134**(6), 307. https://doi.org/10.1140/epjp/i2019-12742-7

Habibi, M., Hashemi, R., Ghazanfari, A., Naghdabadi, R. and Assempour, A. (2018a), "Forming limit diagrams by including the M–K model in finite element simulation considering the effect of bending", *Proceedings of the Institution of Mechanical Engineers, Part L: Journal of Materials: Design and Applications*, **232**(8), 625-636.

Habibi, M., Hashemi, R., Sadeghi, E., Fazaeli, A., Ghazanfari, A. and Lashini, H. (2016), "Enhancing the mechanical properties and formability of low carbon steel with dual-phase microstructures", *J. Mater. Eng. Perform.*, **25**(2), 382-389. https://doi.org/10.1007/s11665-016-1882-1.

Habibi, M., Hashemi, R., Tafti, M.F. and Assempour, A. (2018b), "Experimental investigation of mechanical properties, formability and forming limit diagrams for tailor-welded blanks produced by friction stir welding", *J. Manuf. Proc.*, **31**, 310-323. https://doi.org/10.1016/j.jmapro.2017.11.009.

Habibi, M., Mohammadgholiha, M. and Safarpour, H. (2019b), "Wave propagation characteristics of the electrically GNP-reinforced nanocomposite cylindrical shell", *J. Brazil. Soc. Mech. Sci. Eng.*, **41**(5), 221. https://doi.org/10.1007/s40430-019-1715-x

Habibi, M., Mohammadi, A., Safarpour, H. and Ghadiri, M. (2019c), "Effect of porosity on buckling and vibrational characteristics of the imperfect GPLRC composite nanoshell", *Mech. Based Des. Struct.*, 1-30. https://doi.org/10.1080/15397734.2019.1701490.

Habibi, M., Mohammadi, A., Safarpour, H., Shavalipour, A. and Ghadiri, M. (2019d), "Wave propagation analysis of the laminated cylindrical nanoshell coupled with a piezoelectric actuator", *Mech. Based Des. Struct.*, 1-19. https://doi.org/10.1080/15397734.2019.1697932

Habibi, M., Taghdir, A. and Safarpour, H. (2019e), "Stability analysis of an electrically cylindrical nanoshell reinforced with graphene nanoplatelets", *Compos. Part B Eng.*, **175**, 107125. https://doi.org/10.1016/j.compositesb.2019.107125

Hailong, D., Dan, L., Shaohui, Z. and Yongping, Z. (2018), "A facile approach to synthesize graphitic carbon nitride microwires for enhanced photocatalytic H2 evolution from water splitting under full solar spectrum", *Catal. Sci. Technol.*, **8**, 3599-3609. https://doi.org/10.1039/C8CY00904J

Hammer, B., Hansen, L.B. and Nørskov, J.K. (1999), "Improved adsorption energetics within density-functional theory using revised Perdew-Burke-Ernzerhof functionals", *Phys. Rev. B*, **59**, 7413. https://doi.org/10.1103/PhysRevB.59.7413

Han, M.Y., Oezyilmaz, B., Zhang, Y. and Kim, P. (2007), "Energy band gap engineering of graphene nanoribbons", *Phys. Rev. Lett.*, **98**(20), 206805. https://doi.org/10.1103/PhysRevLett.98.206805

Hao, R.B., Lu, Z.Q., Ding, H. and Chen, L.Q. (2022), "A nonlinear vibration isolator supported on a flexible plate: analysis and experiment", *Nonlinear Dyn.*, **108**(2), 941-958. https://doi.org/10.1007/s11071-022-07243-7

He, X., Wu, Z., Xue, Y., Gao, Z. and Yang, X. (2019), "Fabrication of interlayer β-CD/g-C3N4@MoS2 for highly enhanced photodegradation of glyphosate under simulated sunlight irradiation", *RSC Adv.*, **9**. https://doi.org/10.1039/C8RA10190F

Hong, T., Guo, S., Jiang, W. and Gong, S. (2021), "Highly selective frequency selective surface with ultrawideband rejection", *IEEE T Antennas Propagat.*, **70**(5), 3459-3468. https://doi.org/10.1109/TAP.2021.3137453

Hou, F., Wu, S., Moradi, Z. and Shafiei, N. (2021), "The computational modeling for the static analysis of axially functionally graded micro-cylindrical imperfect beam applying the computer simulation", *Eng. Comput.*, 1-19. https://doi.org/10.1007/s00366-021-01456-x.

Huang, X., Zeng, Z. and Zhang, H. (2013), "Metal dichalcogenide nanosheets: preparation, properties and applications", *Chem. Soc. Rev.*, **42**(5), 1934-1946. https://doi.org/10.1039/C2CS35387C

Huang, X., Zhang, Y., Moradi, Z. and Shafiei, N. (2021a), "Computer simulation via a couple of homotopy perturbation methods and the generalized differential quadrature method for nonlinear vibration of functionally graded non-uniform micro-tube", *Eng. Comput.*, 1-18. https://doi.org/10.1007/s00366-021-01395-7

Huang, X., Zhu, Y., Vafaei, P., Moradi, Z. and Davoudi, M. (2021b), "An iterative simulation algorithm for large oscillation of the applicable 2D-electrical system on a complex nonlinear substrate", *Eng. Comput.*, 1-13. https://doi.org/10.1007/s00366-021-01320-y

Jiao, J., Ghoreishi, S.M., Moradi, Z. and Oslub, K. (2021), "Coupled particle swarm optimization method with genetic algorithm for the static–dynamic performance of the magneto-electro-elastic nanosystem", *Eng. Comput.*, 1-15.

https://doi.org/10.1007/s00366-021-01391-x
Jiao, Y., Ma, F., Gao, G., Bell, J., Frauenheim, T. and Du, A. (2015), "Versatile single-layer sodium phosphidostannate(ii): strain-tunable electronic structure, excellent mechanical flexibility, and an ideal gap for photovoltaics", *J. Phys. Chem. Lett.*, **6**(14), 2682–2687. https://doi.org/10.1021/acs.jpclett.5b01136
Khadimallah, M.A., Hussain, M., Naeem, M.N., Taj, M. and Tounsi, A. (2021a), "Monitoring and control of multiple fraction laws with ring based composite structure", *Adv. Nano Res.*, **10**(2), 129-138. https://doi.org/10.12989/anr.2021.10.2.129
Khadimallah, M.A., Hussain, M., Taj, M., Ayed, H. and Tounsi, A. (2021b), "Parametric vibration analysis of single-walled carbon nanotubes based on Sanders shell theory", *Adv. Nano Res.*, **10**(2), 165-174. https://doi.org/10.12989/anr.2021.10.2.165
King, R.R., Law, D.C., Edmondson, K.M., Fetzer, C.M., Kinsey, G.S., Yoon, H., Sherif, R.A. and Karam, N.H. (2007), "40% efficient metamorphic GaInP⁄GaInAs⁄Ge multijunction solar cells", *Appl. Phys. Lett.*, **90**(18), 510. https://doi.org/10.1063/1.2734507
Kumar, Y., Gupta, A. and Tounsi, A. (2021), "Size-dependent vibration response of porous graded nanostructure with FEM and nonlocal continuum model", *Adv. Nano Res.*, **11**(1), 1-17. https://doi.org/10.12989/anr.2021.11.1.001
Li, J., Shan, Z.-W. and Ma, E. (2014a), "Elastic strain engineering for unprecedented materials properties", *MRS Bull.*, **39**, 108-114. https://doi.org/10.1557/mrs.2014.3
Li, L., Yu, Y., Ye, G.J., Ge, Q., Ou, X., Wu, H., Feng, D., Chen, X.H. and Zhang, Y. (2014b), "Black phosphorus field-effect transistors", *Nature Nanotechnol.*, **9**(5), 372-377. https://doi.org/10.1038/nnano.2014.35
Lin, K.Y.A. and Lin, J.T. (2017), "Ferrocene-functionalized graphitic carbon nitride as an enhanced heterogeneous catalyst of Fenton reaction for degradation of Rhodamine B under visible light irradiation", *Chemosphere*, **182**, 54-64. https://doi.org/10.1016/j.chemosphere.2017.04.152
Liu, J., Xie, C., Dai, X., Jin, L., Zhou, W. and Lieber, C.M. (2013), "Multifunctional three-dimensional macroporous nanoelectronic networks for smart materials", *Proceedings of the National Academy of Sciences of the United States of America*, **110**(17), 6694-6699. https://doi.org/10.1073/pnas.1305209110
Liu, Y., Wang, W., He, T., Moradi, Z. and Larco Benítez, M.A. (2021), "On the modelling of the vibration behaviors via discrete singular convolution method for a high-order sector annular system", *Eng. Comput.*, 1-23. https://doi.org/10.1007/s00366-021-01454-z.
Liu, Z., Su, S., Xi, D. and Habibi, M. (2020), "Vibrational responses of a MHC viscoelastic thick annular plate in thermal environment using GDQ method", *Mech. Based Des. Struct.*, 1-26. https://doi.org/10.1080/15397734.2020.1784201
Luo, J., Song, J., Moradi, Z., Safa, M. and Khadimallah, M.A. (2022), "Effect of simultaneous compressive and inertia loads on the bifurcation stability of shear deformable functionally graded annular fabrications reinforced with graphenes", *Eur. J. Mech. A Solids*, 104581. https://doi.org/10.1016/j.euromechsol.2022.104581
Ma, L., Liu, X. and Moradi, Z. "On the chaotic behavior of graphene-reinforced annular systems under harmonic excitation", *Eng. Comput.*, 1-25. https://doi.org/10.1007/s00366-020-01210-9
Madenci, E. (2021), "Free vibration analysis of carbon nanotube RC nanobeams with variational approaches", *Adv. Nano Res.*, **11**(2), 157-171. https://doi.org/10.12989/anr.2021.11.2.157
Makov, G. and Payne, M.C. (1995), "Periodic boundary conditions in ab initio calculations", *Phys. Rev. B*, **51**(7), 4014. https://doi.org/10.1103/PhysRevB.51.4014
Mccann, E. (2007), "Interlayer asymmetry gap in the electronic band structure of bilayer graphene", *Physica Status Solidi*, **244**. https://doi.org/10.1002/pssb.200776105
Merindol, R. and Walther, A. (2017), "Materials learning from life: Concepts for active, adaptive and autonomous molecular systems", *Chem. Soc. Rev.*, **46**(18), 5588-5619. https://doi.org/10.1039/C6CS00738D
Michael, M., Meyyazhagan, A., Velayudhannair, K., Pappuswamy, M., Maria, A., Xavier, V., Balasubramanian, B., Baskaran, R., Kamyab, H. and Vasseghian, Y. (2022), "The content of heavy metals in cigarettes and the impact of their leachates on the aquatic ecosystem", *Sustainability*, **14**(8), 4752. https://doi.org/10.3390/su14084752
Moradi, Z., Davoudi, M., Ebrahimi, F. and Ehyaei, A.F. (2021), "Intelligent wave dispersion control of an inhomogeneous micro-shell using a proportional-derivative smart controller", *Wave. Random Complex Med.*, 1-24. https://doi.org/10.1080/17455030.2021.1926572
Naumis, G.G., Barraza-Lopez, S., Oliva-Leyva, M. and Terrones, H. (2017), "Electronic and optical properties of strained graphene and other strained 2D materials: A review", *Reports Prog. Phys. Phys. Soc.*, **80**(9), 096501. https://doi.org/10.1088/1361-6633/aa74ef
Novoselov, K.S., Geim, A.K., Morozov, S.V., Jiang, D., Zhang, Y., Dubonos, S.V., Grigorieva, I.V. and Firsov, A.A. (2004), "Electric field effect in atomically thin carbon films", *Science*, **306**(5696), 666-669. https://doi.org/10.1126/science.1102896
O'Connor, J.M. and Casey, C.P. (1987), "Ring-slippage chemistry of transition metal cyclopentadienyl and indenyl complexes", *Chem. Rev.*, **87**(2), 307-318. https://doi.org/10.1021/cr00078a002
Pederson, M.R. and Jackson, K.A. (1991), "Pseudoenergies for simulations on metallic systems", *Phys. Rev. B Condens. Matter.*, **43**(9), 7312-7315. https://doi.org/10.1103/PhysRevB.43.7312
Peng, Y., Zhang, L., Li, Z., Zhong, S., Liu, Y., Xie, S. and Luo, J. (2022), "Influences of wire diameters on output power in electromagnetic energy harvester", *Int. J. Precis. Eng. Manuf. Green Technol.*, 1-12. https://doi.org/10.1007/s40684-022-00446-8
Pourjabari, A., Hajilak, Z.E., Mohammadi, A., Habibi, M. and Safarpour, H. (2019), "Effect of porosity on free and forced vibration characteristics of the GPL reinforcement composite nanostructures", *Comput. Math. Appl.*, **77**(10), 2608-2626. https://doi.org/10.1016/j.camwa.2018.12.041.
Rocha, A.R., García-Suárez, V.M., Bailey, S.W., Lambert, C.J. and Sanvito, S. (2006), "Spin and molecular electronics in atomically generated orbital landscapes", *Phys. Rev. B*, **73**(8), 085414 . https://doi.org/10.1103/PhysRevB.73.085414
Roldán, R., Castellanos-Gomez, A., Cappelluti, E. and Guinea, F. (2015), "Strain engineering in semiconducting two-dimensional crystals", *J. Phys. Conden. Matter.*, **27**(31), 313201. https://doi.org/10.1088/0953-8984/27/31/313201
Rungger, I. and Sanvito, S. (2008), "Algorithm for the construction of self-energies for electronic transport calculations based on singularity elimination and singular value decomposition", *Phys. Rev. B*, **78**(3), 1436-1446. https://doi.org/10.1103/PhysRevB.78.035407
Safarpour, H., Ghanizadeh, S.A. and Habibi, M. (2018), "Wave propagation characteristics of a cylindrical laminated composite nanoshell in thermal environment based on the nonlocal strain gradient theory", *Eur. Phys. J. Plus*, **133**(12), 532. https://doi.org/10.1140/epjp/i2018-12385-2.
Safarpour, H., Hajilak, Z.E. and Habibi, M. (2019a), "A size-dependent exact theory for thermal buckling, free and forced vibration analysis of temperature dependent FG multilayer GPLRC composite nanostructures restring on elastic foundation", *Int. J. Mech. Mater. Des.*, **15**(3), 569-583.

https://doi.org/10.1007/s10999-018-9431-8.
Safarpour, H., Pourghader, J. and Habibi, M. (2019b), "Influence of spring-mass systems on frequency behavior and critical voltage of a high-speed rotating cantilever cylindrical three-dimensional shell coupled with piezoelectric actuator", *J. Vib. Control*, **25**(9), 1543-1557. https://doi.org/10.1177/1077546319828465
Safarpour, M., Ebrahimi, F., Habibi, M. and Safarpour, H. (2020), "On the nonlinear dynamics of a multi-scale hybrid nanocomposite disk", *Eng. Comput.*, 1-20. https://doi.org/10.1007/s00366-020-00949-5
Schwierz, F. (2010), "Graphene transistors", *Nature Nanotechnol.*, **5**(7), 487-496. https://doi.org/10.1038/nnano.2010.89
Shao, Y., Zhao, Y., Gao, J. and Habibi, M. (2021), "Energy absorption of the strengthened viscoelastic multi-curved composite panel under friction force", *Arch. Civil Mech. Eng.*. **21**(4), 1-29. https://doi.org/10.1007/s43452-021-00279-3
Shariati, M., Kamyab, H., Habibi, M., Ahmadi, S., Naghipour, M., Gorjinezhad, F., Mohammadirad, S and Aminian, A. (2023), "Sulfuric acid resistance of concrete containing coal waste as a partial substitute for fine and coarse aggregates", *Fuel*, **348**, 128311. https://doi.org/10.1016/j.fuel.2023.128311
Sharma, P., Ganti, S. and Bhate, N. (2003), "Effect of surfaces on the size-dependent elastic state of nano-inhomogeneities", *Appl. Phys. Lett.*, **82**(4), 535-537. https://doi.org/10.1063/1.1539929
Shengchun, Yang, Fuzhu, Liu, Chao, Wu, Sen and Yang (2016), "Tuning surface properties of low dimensional materials via strain engineering", *Small*, **12**(30), 4028-4047. https://doi.org/10.1002/smll.201601203
Shi, D., Chen, Y., Li, Z., Dong, S., Li, L., Hou, M., Liu, H., Zhao, S., Chen, X. and Wong, C.P. (2022), "Anisotropic charge transport enabling high-throughput and high-aspect-ratio wet etching of silicon carbide", *Small Methods*, 2200329. https://doi.org/10.1002/smtd.202200329
Shockley, W. and Queisser, H.J. (1961), "Detailed balance limit of efficiency of P-N junction solar cells", *J. Appl. Phys.*, **32**(3), 510-519. https://doi.org/10.1063/1.1736034
Tan, C. and Zhang, H. (2015), "Two-dimensional transition metal dichalcogenide nanosheet-based composites", *Chem. Soc. Rev.*, **44**(9), 2713-2731. https://doi.org/10.1039/C4CS00182F
Testing, A.S.f., Weathering, M.C.G.o. and Durability (2008), *Standard Tables for Reference Solar Spectral Irradiances: Direct Normal and Hemispherical on 37° Tilted Surfaces*, Springer, England.
Thomas, A., Fischer, A., Goettmann, F., Antonietti, M., Müller, J. O., Schlögl, R. and Carlsson, J.M. (2008), "Graphitic carbon nitride materials: variation of structure and morphology and their use as metal-free catalysts", *J. Mater. Chem.*, **18**(41), 4893-4908. https://doi.org/10.1039/B800274F
Tlidji, Y., Benferhat, R., Trinh, L.C., Tahar, H.D. and Abdelouahed, T. (2021), "New state-space approach to dynamic analysis of porous FG beam under different boundary conditions", *Adv. Nano Res.*, **11**(4), 347-359. https://doi.org/10.12989/anr.2021.11.4.347
Topsakal, M., Aktuerk, E. and Ciraci, S. (2009), "First-principles study of two- and one-dimensional honeycomb structures of boron nitride", *Phys. Rev. B*, **79**(11), 115442. https://doi.org/10.1103/PhysRevB.79.115442
Tsai, H., Nie, W., Blancon, J.C., Stoumpos, C.C., Asadpour, R., Harutyunyan, B., Neukirch, A.J., Verduzco, R., Crochet, J.J., Tretiak, S., Pedesseau, L., Even, J., Alam, M.A., Gupta, G., Lou, J., Ajayan, P.M., Bedzyk, M.J. and Kanatzidis, M.G. (2016), "High-efficiency two-dimensional Ruddlesden-Popper perovskite solar cells", *Nature*, **536**(7616), 312-316. https://doi.org/10.1038/nature18306
Veiros and Luis, F. (2012), "Haptotropic shifts in cyclopentadienyl organometallic complexes: Ring folding vs ring slippage", *Organometallics*, **19**(26), 5549-5558. https://doi.org/10.1021/om000589a
Wang, H., Habibi, M., Marzouki, R., Majdi, A., Shariati, M., Denic, N., Zakić, A., Khorami, M., Khadimallah, M.A. and Ebid, A.A.K. (2022a), "Improving the self-healing of cementitious materials with a hydrogel system", *Gels*. **8**(5), 278. https://doi.org/10.3390/gels8050278
Wang, L., Sofer, Z. and Pumera, M. (2020a), "Will any crap we put into graphene increase its electrocatalytic effect?", *ACS Nano*, **14**(1). https://doi.org/10.1021/acsnano.9b00184
Wang, Y., Yang, J., Moradi, Z., Safa, M. and Khadimallah, M.A. (2022b), "Nonlinear dynamic analysis of thermally deformed beams subjected to uniform loading resting on nonlinear viscoelastic foundation", *Eur. J. Mech. A Solids*, **95**, 104638. https://doi.org/10.1016/j.euromechsol.2022.104638
Wang, Z., Yu, S., Xiao, Z. and Habibi, M. (2020b), "Frequency and buckling responses of a high-speed rotating fiber metal laminated cantilevered microdisk", *Mech. Adv. Mater. Struct.*, 1-14. https://doi.org/10.1080/15376494.2020.1824284
Wu, J. and Habibi, M. (2021), "Dynamic simulation of the ultra-fast-rotating sandwich cantilever disk via finite element and semi-numerical methods", *Eng. Comput.*, 1-17. https://doi.org/10.1007/s00366-021-01396-6
Wu, Y., Zhao, Y., Han, X., Jiang, G., Shi, J., Liu, P., Khan, M.Z., Huhtinen, H., Zhu, J. and Jin, Z. (2021), "Ultra-fast growth of cuprate superconducting films: dual-phase liquid assisted epitaxy and strong flux pinning", *Mater. Today Phys.*, **18**, 100400. https://doi.org/10.1016/j.mtphys.2021.100400
Xi, Y., Jiang, W., Wei, K., Hong, T., Cheng, T. and Gong, S. (2021), "Wideband RCS reduction of microstrip antenna array using coding metasurface with low Q resonators and fast optimization method", *IEEE Antennas Wireless Propagat. Lett.*, **21**(4), 656-660. https://doi.org/10.1109/LAWP.2021.3138241
Xia, W., Du, J., Habibi, M., Shariati, M. and Khadimallah, M.A. (2022), "Application of Chebyshev-based GDQ and Newmark methods to viscothermoelasticity responses of FG composite annular systems", *Eng. Anal. Bound. Elem.*, **143**, 28-42. https://doi.org/10.1016/j.enganabound.2022.06.003
Xin, C., Li, Z., Zhang, Q., Peng, Y., Guo, H. and Xie, S. (2022), "Investigating the output performance of Triboelectric Nanogenerators with Single/Double-sided interlayer", *Nano Energy*, 107448. https://doi.org/10.1016/j.nanoen.2022.107448
Xu, K.D., Weng, X., Li, J., Guo, Y.J., Wu, R., Cui, J. and Chen, Q. (2022), "60-GHz third-order on-chip bandpass filter using GaAs pHEMT technology", *Semiconduct. Sci. Technol.*, **37**(5), 055004. https://doi.org/10.1088/1361-6641/ac5bf8
Xu, W., Pan, G., Moradi, Z. and Shafiei, N. (2021), "Nonlinear forced vibration analysis of functionally graded non-uniform cylindrical microbeams applying the semi-analytical solution", *Compos. Struct.*, 114395. https://doi.org/10.1016/j.compstruct.2021.114395
Yang, M., Li, C., Said, Z., Zhang, Y., Li, R., Debnath, S., Ali, H.M., Gao, T. and Long, Y. (2021), "Semiempirical heat flux model of hard-brittle bone material in ductile microgrinding", *J. Manuf. Proc.*, **71**, 501-514. https://doi.org/10.1016/j.jmapro.2021.09.053
Yang, N., Moradi, Z., Khadimallah, M.A. and Arvin, H. (2022), "Application of the Chebyshev–Ritz route in determination of the dynamic instability region boundary for rotating nanocomposite beams reinforced with graphene platelet subjected to a temperature increment", *Eng. Anal. Bound. Elem.*, **139**, 169-179. https://doi.org/10.1016/j.enganabound.2022.03.013
Ye, X., Zheng, Y. and Wang, X. (2014), "Synthesis of ferrocene-modified carbon nitride photocatalysts by surface amindation reaction for phenol synthesis", *Chinese J. Chem.*, **32**(006), 498-506. https://doi.org/10.1002/cjoc.201400229

Yoshikawa, K., Kawasaki, H., Yoshida, W., Irie, T., Konishi, K., Nakano, K., Uto, T., Adachi, D., Kanematsu, M. and Uzu, H. (2017), "Silicon heterojunction solar cell with interdigitated back contacts for a photoconversion efficiency over 26%", *Nature Energy*, **2**, 17032. https://doi.org/10.1038/nenergy.2017.32

Yu, X., Maalla, A. and Moradi, Z. (2022), "Electroelastic high-order computational continuum strategy for critical voltage and frequency of piezoelectric NEMS via modified multi-physical couple stress theory", *Mech. Syst. Signal Pr.*, **165**, 108373. https://doi.org/10.1016/j.ymssp.2021.108373.

Zhang, T., Jin, Y., Shi, Y., Li, M., Li, J. and Duan, C. (2019), "Modulating photoelectronic performance of metal–organic frameworks for premium photocatalysis", *Coordinat. Chem. Rev.*, **380**, 201-229. https://doi.org/10.1016/j.ccr.2018.10.001

Zhao, Y., Moradi, Z., Davoudi, M. and Zhuang, J. "Bending and stress responses of the hybrid axisymmetric system via state-space method and 3D-elasticity theory", *Eng. Comput.*, 1-23. https://doi.org/10.1007/s00366-020-01242-1

Zheng, H., Liu, G., Zhu, L., Ye, J., Zhang, X., Alsaedi, A., Hayat, T., Pan, X. and Dai, S. (2018), "The effect of hydrophobicity of ammonium salts on stability of quasi-2D perovskite materials in moist condition", *Adv. Energy Mater.*, **8**(21), 1800051.1800051-1800051.1800058. https://doi.org/10.1002/aenm.201800051

Zhi, C., Bando, Y., Tang, C., Kuwahara, H. and Golberg, D. (2009), "Large-scale fabrication of boron nitride nanosheets and their utilization in polymeric composites with improved thermal and mechanical properties", *Adv. Mater.*, **21**(28), 2889-2893. https://doi.org/10.1002/adma.200900323

Zhou, C., Zhao, Y., Zhang, J., Fang, Y. and Habibi, M. (2020), "Vibrational characteristics of multi-phase nanocomposite reinforced circular/annular system", *Adv. Nano Res.*, **9**(4), 295-307. https://doi.org/10.12989/anr.2020.9.4.295

Zhou, N., Shen, Y., Li, L., Tan, S., Liu, N., Zheng, G., Chen, Q. and Zhou, H. (2018), "Exploration of crystallization kinetics in quasi two-dimensional perovskite and high performance solar cells", *J. Am. Chem. Soc.*, **140**(1), 459. https://doi.org/10.1021/jacs.7b11157

Zhou, Y., Zhang, L., Liu, J., Fan, X., Wang, B., Wang, M., Ren, W., Wang, J., Li, M. and Shi, J. (2015), "Brand new P-doped g-C3N4: Enhanced photocatalytic activity for H2 evolution and Rhodamine B degradation under visible light", *J. Mater. Chem. A*, **3**(7), 3862-3867. https://doi.org/10.1039/C4TA05292G

Zhu, B., Zhang, L., Cheng, B. and Yu, J. (2018), "First-principle calculation study of tri-s-triazine-based g-C3N4: A review", *Appl. Catal. B Environ.*, **224**, 983-999. https://doi.org/10.1016/j.apcatb.2017.11.025

Zhu, L., Ren, H., Habibi, M., Mohammed, K.J. and Khadimallah, M.A. (2022), "Predicting the environmental economic dispatch problem for reducing waste nonrenewable materials via an innovative constraint multi-objective Chimp Optimization Algorithm", *J. Clean. Prod.*, 132697. https://doi.org/10.1016/j.jclepro.2022.132697

Zupan, A., Burke, K., Ernzerhof, M. and Perdew, J.P. (1997), "Distributions and averages of electron density parameters: Explaining the effects of gradient corrections", *J. Chem. Phys.*, **106**(24), 10184-10193. https://doi.org/10.1063/1.474101